Adducts of Cyclotriphosphorus Complexes with Cyclopentadienyl Ruthenium Fragments: Synthesis, Solid-State Structure and Solution Behaviour

Pierluigi Barbaro,[b] Massimo Di Vaira,[a] Maurizio Peruzzini,[b] Stefano Seniori Costantini,[a] and Piero Stoppioni*[a]

Keywords: Cyclotriphosphorus / Ruthenium / Cyclopentadienyl / Monodentate P ligands

Treatment of the cyclo-P_3 complexes [(triphos)M(η^3-P_3)]-[triphos = 1,1,1-tris(diphenylphosphanylmethyl)ethane; M = Co (**1**), Rh (**2**)] with stoichiometric amounts of [CpRu-$(CH_3CN)_2(PR_3)$]PF_6 [R = Ph (**3**), Me (**4**), Cy (**5**)] in CH_2Cl_2 in the presence of CH_3CN yields the bimetallic adducts [{(triphos)M}($\mu,\eta^{3:1}$-P_3){CpRu(CH_3CN)(PR_3)}]PF_6 [M = Co; R = Ph (**6**), Me (**7**), Cy (**8**); M = Rh; R = Ph, (**9**), Me (**10**), Cy (**11**)]. The rhodium derivatives **9** and **11**, upon treatment with one equivalent of PMe_3, form the complexes [{(triphos)Rh}($\mu,\eta^{3:1}$-P_3){CpRu(PMe_3)(PR_3}]PF_6 [R = Ph (**12**), Cy (**13**)]. On standing in CH_2Cl_2, the rhodium complexes **9** and **10** lose acetonitrile to yield compounds with the formula [{(triphos)Rh}($\mu,\eta^{3:1,1'}$-P_3){CpRu(PR_3)}]PF_6 [R = Ph (**14**), Me (**15**)]. All the compounds have been characterised by elemental analyses and, in solution, by ^{31}P and ^1H NMR spectroscopy. The $^{31}P\{^1H\}$ EXSY NMR spectroscopic data at different temperatures of **11** and **14** have highlighted the occurrence of independent dynamic processes that exchange both the triphos and the cyclo-P_3 phosphorus nuclei. An X-ray structural investigation carried out on **6** has confirmed the occurrence of the $\mu,\eta^{3:1}$-ligating behaviour of the cyclo-P_3 ligand.

Introduction

"Naked" group 15 ligands stabilised by transition-metal moieties exhibit lone pair electrons, owing to which they are generally endowed with reactivity toward metal fragments with Lewis acid character. Many compounds have been described that result from the addition of metal moieties, mainly carbonyl or cyclopentadienyl carbonyl metal fragments, to the above metal-supported main group atom ligands. The added moieties, depending on their ligating properties, may bind in η^1-, η^2- or η^3 fashion to the main group units to afford bi-, tri- and tetrametallic complexes.[1–5] The solution structures of these multimetallic adducts may usually be assigned by in-depth ^{31}P NMR spectroscopic studies. These NMR studies have often revealed the occurrence of a dynamic behaviour consisting of (i) skeleton rearrangements of multinuclear cluster compounds,[6–12] (ii) relative rotation of parts of the molecule about symmetry- or pseudosymmetry axes,[13–16] and (iii) scrambling of coordinated fragments.[17,18] In our laboratories the reactivity of a series of neutral[19–21] and cationic[22–25] complexes has been investigated, in which a cyclic triatomic E_3 or E_2X (E = P, As; X = S, Se) group isη^3 bound to a metal atom of the cobalt or of the nickel group and is supported by the tripodal tridentate 1,1,1-tris(diphenylphosphanylmethyl)ethane (triphos) ligand (Scheme 1).[26,27]

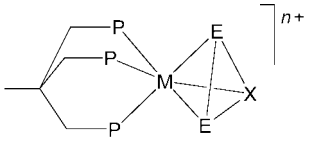

n = 0 M = Co, Rh, Ir; E = X = P

n = 1 M = Ni, Pd, Pt; E = X = P

n = 1 M = Co; E = P, As; X = S, Se

Scheme 1.

The neutral compounds [(triphos)M(η^3-P_3)] (M = Co, Rh) easily add coordinatively unsaturated metal fragments, such as $M(CO)_5$ (M = Cr, W) or $CpMn(CO)_2$, to yield bi-, tri- and tetrametallic adducts in which the geometry of the P_3 ring is only slightly modified from that in the parent compounds.[19,21,28–31] In contrast, the cationic [(triphos)-M(η^3-E_2X)]$^+$ species (M = Ni; E = X = P. M = Co; E = P, As; X = S, Se) do not add carbonyl fragments, but readily insert the 14e $M(PPh_3)_2$ (M = Pd, Pt) carbene-like moieties into an E–E or E–X bond of the triatomic ring.[31–33] Interestingly, all of these polymetallic compounds exhibit dynamic behaviour at room temperature. Recent studies on a series of complexes resulting from the addition of one me-

[a] Dipartimento di Chimica, Università di Firenze, via della Lastruccia, 3, 50019 Sesto Fiorentino, Firenze, Italy
[b] ICCOM-CNR, via Madonna del Piano snc, 50019 Sesto Fiorentino, Firenze, Italy

tal-carbonyl fragment to [(triphos)M(η^3-P_3)] (M = Co, Rh) have definitely shown that two fluxional processes occur in solution, i.e. the scrambling of the metal-carbonyl moiety over the P_3 cyclic system and the relative rotation of the P_3 and {(triphos)M} moieties about their common C_3 axis.[34] Variable-temperature NMR analysis has also established that the rhodium derivatives have a higher rotational barrier than the cobalt derivatives.[34] The scrambling process over cyclo-P_3, which has been blocked at low temperature for both cobalt and rhodium derivatives, has a higher barrier with respect to the {(triphos)M} rotation. Indeed, the latter process has been blocked on the NMR time scale only for the rhodium adduct [{(triphos)Rh}($\mu,\eta^{3:1}$-P_3){$W(CO)_4$-PPh_3}], which is formed with the sterically demanding $W(CO)_4(PPh_3)$ fragment sitting as an end-on ligand on the cyclotriphosphorus unit.[34]

In this work we have investigated the reactivity of [(triphos)M(η^3-P_3)] [M = Co (**1**), Rh(**2**)] toward the [$CpRu(CH_3CN)_2(PR_3)$]PF_6 [R = Ph (**3**), Me (**4**), Cy (**5**)] complexes. These species contain two acetonitrile molecules that can be selectively replaced to generate the 16e [$CpRu(CH_3CN)(PR_3)$]$^+$ and 14e [$CpRu(PR_3)$]$^+$ fragments, respectively.[35] The 16e moieties appear to be particularly suitable, upon reaction with **1** and **2**, to provide further information on the factors affecting the scrambling process of the metal fragment, as they are more sterically hindered than the carbonyl moieties previously employed and, furthermore, their steric demand may be varied by changing the phosphane substituents. Moreover, the lability of the second acetonitrile molecule may further extend the reactivity of the P_3 ring, already activated by the initial end-on coordination of the ruthenium fragment.

Results and Discussion

The dinuclear compounds with the formula [{(triphos)M}($\mu,\eta^{3:1}$-P_3){$CpRu(CH_3CN)(PR_3)$}]PF_6 [M = Co; R = Ph (**6**), Me (**7**), Cy (**8**); M = Rh; R = Ph, (**9**), Me (**10**), Cy (**11**)] are obtained in a straightforward manner by adding a stoichiometric amount of the appropriate [$CpRu(CH_3CN)_2(PR_3)$]PF_6 complex to [(triphos)M(η^3-P_3)] [M = Co (**1**), Rh (**2**)] dissolved in CH_2Cl_2 in the presence of CH_3CN (see the Experimental Section). The complexes **6–11** can be regarded as the mono adducts of the cyclo-P_3 unit in **1** or **2** with 16e [$CpRu(CH_3CN)(PR_3)$]$^+$ (R = Ph, Me, Cy) fragments that readily result from the removal of one labile acetonitrile molecule from [$CpRu(CH_3CN)_2(PR_3)$]PF_6 (Scheme 2). The concentration of CH_3CN is crucial for obtaining **6–11** in both high yield and purity. Actually, **1** and **2** do not react with the ruthenium complexes under conditions of high CH_3CN concentration, which hamper the substitution of the coordinating molecule that occurs through a dissociative pathway.[35] The complexes **6–11** may be handled in air for a limited time; they are soluble in polar organic solvents and their solutions are stable in an inert atmosphere. Solutions of **6–11**, in both $(CH_3)_2CO$ or $CHCl_3$, decompose when heated to 40–50 °C, yielding a mixture of compounds, which could not be characterised.

X-ray Structure Analysis

The structure of **6**, determined by X-ray crystal analysis, consists of [{(triphos)Co}($\mu,\eta^{3:1}$-P_3){$CpRu(CH_3CN)(PPh_3)$}]$^+$ cations (Figure 1), PF_6^- anions, and toluene solvate molecules in a 1:1:2 ratio. Selected values of bond

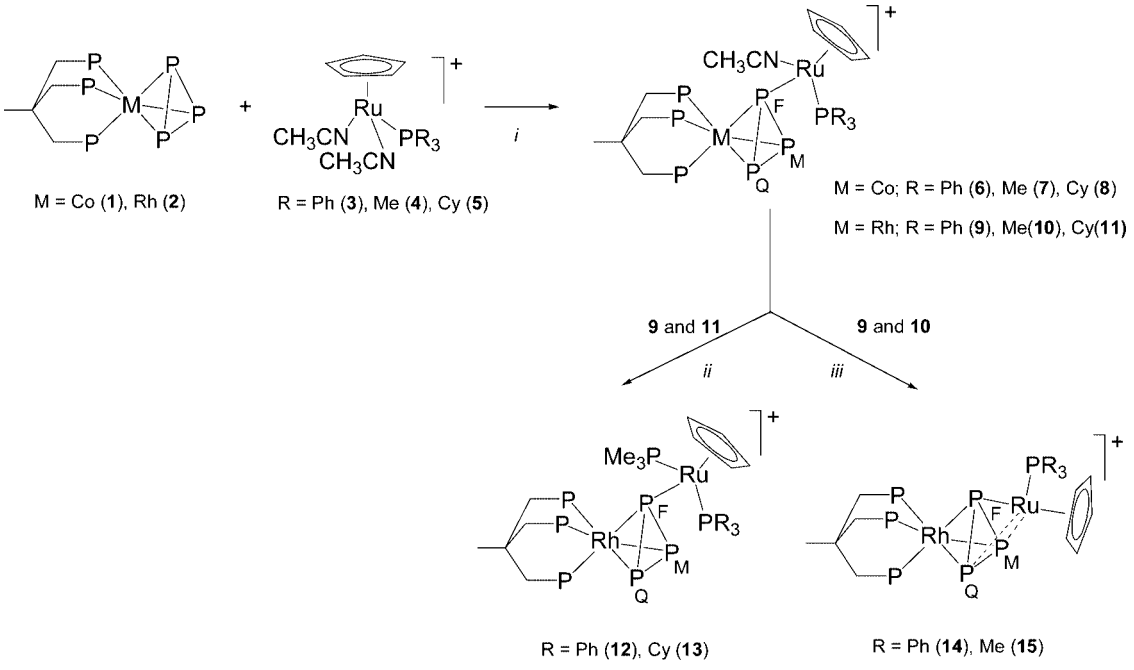

Scheme 2. *i*) CH_3CN, CH_2Cl_2, toluene; *ii*) CH_2Cl_2, PMe_3, toluene; *iii*) CH_2Cl_2, toluene.

lengths and angles are given in Table 1. In the dimetal cation, the {CpRu(CH_3CN)(PPh_3)} moiety forms through its metal atom an end-on monoadduct on a phosphorus atom of the CoP_3 core. Such a pseudotetrahedral core exhibits some deviations from the regular geometry of the parent compound **1**, consisting of (i) a moderately shorter Co–P bond formed by the bridging phosphorus atom [P(5)] between the two metal atoms, with respect to the other two Co–P bonds, and (ii) slightly shorter P–P bonds formed by the same P(5) atom than the third P–P bond in the P_3 unit. Consistent deviations from regularity have been detected for metal carbonyl monoadducts of **1** and **2**[34] and similar, although more pronounced, deviations have been found for a methyl adduct.[36] Rationalizations for these trends have already been proposed.[13,34]

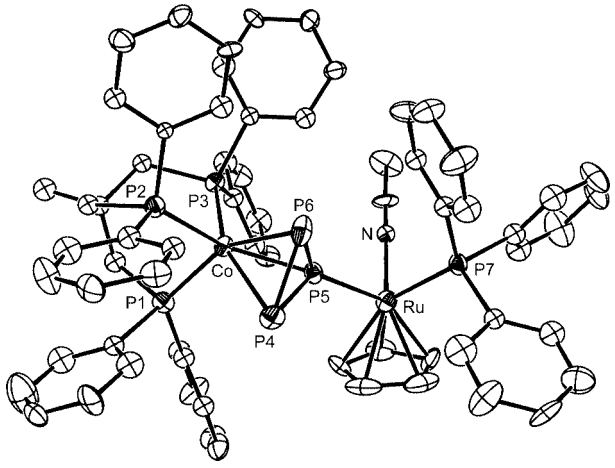

Figure 1. A view of the [{(triphos)Co}(μ,$\eta^{3:1}$-P_3)-{CpRu(CH_3CN)(PPh_3)}]$^+$ cation in the structure of **6**; displacement ellipsoids traced at the 20 % probability level. H atoms are not shown and labels for the carbon atoms are omitted for clarity.

Table 1. Selected bond lengths [Å] and bond angles [°] for **6**.

Bond lengths			
Co–P(1)	2.178(5)	P(4)–P(6)	2.142(6)
Co–P(2)	2.200(5)	P(5)–P(6)	2.100(5)
Co–P(3)	2.209(5)	Ru–P(5)	2.353(4)
Co–P(4)	2.316(5)	Ru–N	2.025(12)
Co–P(5)	2.273(5)	Ru–P(7)	2.325(4)
Co–P(6)	2.333(5)	Ru–Ct[a]	1.849
P(4)–P(5)	2.117(6)		
Bond angles			
P(1)–Co–P(2)	90.4(2)	P(5)–Ru–P(7)	95.5(2)
P(1)–Co–P(3)	96.1(2)	P(5)–Ru–N	94.6(3)
P(2)–Co–P(3)	90.6(2)	P(7)–Ru–N	88.9(3)
P(4)–Co–P(5)	54.9(2)	N–Ru–Ct[a]	124.8
P(4)–Co–P(6)	54.9(2)	P(5)–Ru–Ct[a]	120.2
P(5)–Co–P(6)	54.2(2)	P(7)–Ru–Ct[a]	124.3
Co–P(5)–Ru	156.9(2)		

[a] Distance and angles formed by the centroid (Ct) of the Cp ring. The Ru–C(Cp) distances are in the range 2.195–2.224 Å.

The ruthenium atom forms a slightly longer bond to the P_3 phosphorus atom than to the phosphane donor atom (Table 1). These two P atoms and the CH_3CN nitrogen atom substantially span a face of an octahedron around the ruthenium atom; the opposite side of the coordination sphere is occupied by the cyclopentadienyl ligand. A similar coordination geometry, although in this case the nitrogen atom of a second CH_3CN ligand replaces the P_3 phosphorus atom, has recently been found for a ruthenium derivative, in which the Ru–P(phosphane) and Ru–C(Cp) mean distances are marginally shorter than the present ones and both Ru–N distances are longer by 0.05 Å.[37]

NMR Properties of the Compounds

The room temperature $^{31}P\{^1H\}$ NMR spectra of the compounds **6–11** recorded in CD_2Cl_2 show resonances that fall into two quite distinct regions: a group of signals at low field (50–2 ppm) is assigned to the phosphorus atoms of triphos and of the phosphane bound to ruthenium (see Experimental Section), while a second group of high-field shifted signals (from –150 to –304 ppm) is assigned to the "naked" P atoms from the cyclo-P_3 ligand. Table 2 presents the NMR spectroscopic data for the latter resonances, and the relevant labelling scheme is shown in Scheme 2. The intensity ratios of the signals agree with the proposed formulae. The resonance for the triphos phosphorus atoms exhibits chemical shifts that are similar to those of the parent [(triphos)M(η^3-P_3)] [M = Co (**1**) and Rh (**2**)][22] compounds and of other end-on carbonyl adducts.[13,34] The phosphorus atom of the PR_3 ligand yields a doublet due to coupling with P_F; both the chemical shift and the coupling constant of the phosphane ligand are in the range observed for [CpRu(PR_3)(PR_3')(L)] complexes.[38] This could indirectly suggest that the donor/acceptor properties of the "naked" phosphorus atoms in the "ligand" [(triphos)M(η^3-P_3)] should be similar to those of the phosphanes. Signals due to the P atoms of the cyclo-P_3 unit are split into three distinct multiplets in the high-field region with integral ratios of 1:1:1. Irrespective of the compound, the signal at lower field appears as a triplet, while the other two, occurring at higher field, consist each of a doublet of doublets, with small differences in their chemical shifts. The overall high-field shifts of the P atoms involved in the cyclo-P_3 ring clearly suggest that this unit has undergone only minor modifications upon coordination to the ruthenium fragment. Indeed, severe rearrangements of the cyclic unit, such as cleavage of one of its P–P bonds, significantly affect the chemical shifts, which move to low field with respect to the signal of the parent compound.[32] The multiplicities of the resonances under discussion allow the safe assignment of the low-field triplet to P_F, which is slightly deshielded by coordination to the ruthenium fragment. Consequently, the two high-field resonances may be safely assigned to the two phosphorus atoms P_M and P_Q that are not coordinated to ruthenium. Such an assignment is strongly supported by the analogous shifts observed in the low-temperature ^{31}P NMR spectra of the monoadducts of [(triphos)M(η^3-P_3)] with metal carbonyl fragments.[34] It is worth noting that while the resonance of the end-on Ru-coordinated P_F atom undergoes a low-field shift with respect to that observed for the parent [(triphos)-

Table 2. $^{31}P\{^1H\}$ NMR spectroscopic data at room temperature for the "naked" P atoms of the compounds **6–15**.

Compound[a]	Chemical shift, δ [ppm]			Coupling constant, J [Hz]	
	P_F	P_M or P_Q	P_Q or P_M	$^1J(P_F\text{-}P_M) = {}^1J(P_F\text{-}P_Q)$	$^1J(P_M\text{-}P_Q)$
6	–175.7 (tbr)	–290.8 (ddbr)	–301.5 (ddbr)	320.0	264.0
7	–164.6 (tbr)	–291.8 (ddbr)	–306.8 (ddbr)	320.0	256.0
8	–187.9 (tbr)	–283.6 (ddbr)	–296.0 (ddbr)	321.0	260.0
9	–164.4 (tm)	–284.9 (ddm)	–297.8 (ddm)	337.0	265.0
10	–159.7 (tm)	–288.7 (ddm)	–303.6 (ddm)	338.0	257.0
11	–173.2 (tm)	–278.5 (ddm)	–293.7 (ddm)	335.0	258.0
12	–179.1 (tm)	–269.9 (ddm)	–274.4 (ddm)	340.0	256.0
13	–180.0 (tm)	–267.5 (ddm)	–274.9 (ddm)	330.0	259.0
14	–164.7 (tbr)	–259.1 (ddbr)	–270.9 (ddbr)	303.0	252.0
15	–151.5 (tbr)	–276.7 (dbr)	–276.7 (dbr)	320.0	0

[a] The NMR spectra were recorded in CD_2Cl_2 with a Varian Gemini g300bb spectrometer. Key: d = doublet, t = triplet, m = multiplet, br = broad. The cyclo-P_3 in the parent compounds [(triphos)M(P_3)] yields a broad singlet (δ = –276.2 ppm) for M = Co (**1**) and a doubled quartet [δ = –261.0, ^1J(P–Rh) 13, $^2J(P\text{–}P_{triphos})$ 12 Hz] for M = Rh (**2**).

M(η^3-P_3)] compound, the P_M and P_Q resonances move high field, suggesting an increase of local electron density upon coordination of the ruthenium moiety to the cobalt or rhodium cyclo-P_3 starting material. The inequivalence of P_M and P_Q, that is observed for all of the complexes irrespective of the phosphane substituent, may be ascribed to the chirality of the $[CpRu(CH_3CN)(PR_3)]^+$ fragment, although different environments of the two P atoms are likely to result also from the effects of steric repulsions between the phenyl ends of the {(triphos)M} moiety and the ruthenium fragment. The ^1J coupling constants between P_F, P_M, and P_Q lie in the range spanned by other end-on adducts of cyclo-P_3.[34] Both the triphos and "naked" P atom signals of the cobalt derivatives **6–8** are broadened by the cobalt quadrupole, so that only the largest ^1J coupling constants between the unsubstituted P atoms may be detected. The rhodium complexes **9–11** exhibit broad signals for the triphos P atoms, but sharp patterns for the "naked" phosporus nuclei. Such data point to the occurrence at room temperature of a dynamic process, on the NMR time scale, that involves motion of the triphos ligand with respect to a fixed frame formed by the "naked P" atoms. On the other hand, no dynamic process involving the scrambling motion of the Ru-metal moiety over the P_3 cyclic system is observed at room temperature for **6–11**, irrespective of large differences in the steric requirements of the PR_3 phosphanes employed. This is in contrast with the behaviour of the metal carbonyls previously investigated,[34] which exhibited dynamic behaviour at room temperature, and this suggests that such differences may be influenced by electronic factors, rather than by steric ones. The decomposition of the complexes upon warming their solutions prevented a through investigation of possible dynamic processes involving the Ru-metal moiety and the P_3 cyclic system at higher temperatures. However, the dynamic behaviour of **11** has been carefully investigated at various temperatures by means of ^1H, $^{31}P\{^1H\}$ and 2D $^{31}P\{^1H\}$ EXSY spectroscopic analyses. Sections of selected variable-temperature $^{31}P\{^1H\}$ spectra are shown in Figure 2.

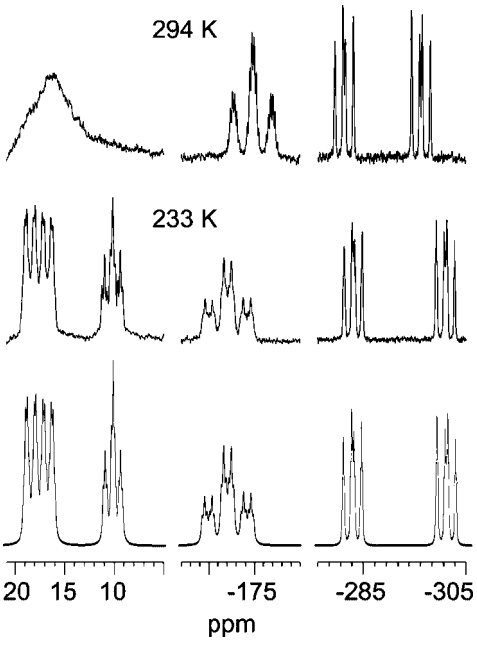

Figure 2. Sections of the $^{31}P\{^1H\}$ NMR spectra of **11** (CD_2Cl_2, 161.95 MHz). Top, experimental spectrum at 294 K; middle, experimental spectrum at 233 K; bottom, simulated spectrum at 233 K. The resonances due to the PCy_3 phosphorus are omitted for clarity.

The rate of the exchange of triphos donor atoms is lowered on cooling the solution. In particular, at 233 K, the triphos phosphorus atoms exhibit separated multiplets centred at 18.45, 16.75 and 10.18 ppm, with coupling constants that range from 29.5 to 130.0 Hz (data obtained by computer simulation) (Table 3). The $^{31}P\{^1H\}$ EXSY spectra recorded at 294 and 248 K are reported in Figure 3. Indeed, two distinct sets of exchange peaks are observed, showing that **11** attains an overall slow motional regime in the above temperature range.[39] A set of exchange peaks is detected at temperatures higher than 260 K, and is relative to the high-field signals due to P_3 (Figure 3, top); the other set, that can be observed below the coalescence point, connects the resonances of the triphos phosphorus atoms (Figure 3, bottom).

This exchange pattern is consistent with the existence of two distinct dynamic processes that have different activation energies; the energy for the process for the P_3 exchange is higher than that for the other one. Such dynamic behaviour

Table 3. $^{31}P\{^{1}H\}$ NMR spectroscopic data of compound **11**[a].

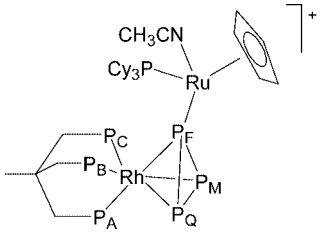

Nucleus	δ [ppm]	Coupling constants J_{PP} [Hz]						J_{PRh} [Hz]
		P_B	P_C	P_F	P_M	P_Q	PCy_3	
P_A	10.18	33.2	29.5	130.0	0.0	0.0	0.0	130.2
P_B	16.75		29.5	0.0	31.0	0.0	0.0	134.3
P_C	18.45			0.0	0.0	29.5	0.0	138.5
P_F	–172.11				336.3	343.8	42.7	43.0
P_M	–282.16					257.2	0.0	32.2
P_Q	–300.78						0.0	30.5
PCy_3	44.46							0.0

[a] In CD_2Cl_2, 161.95 MHz, 233 K. Data by computer simulation.

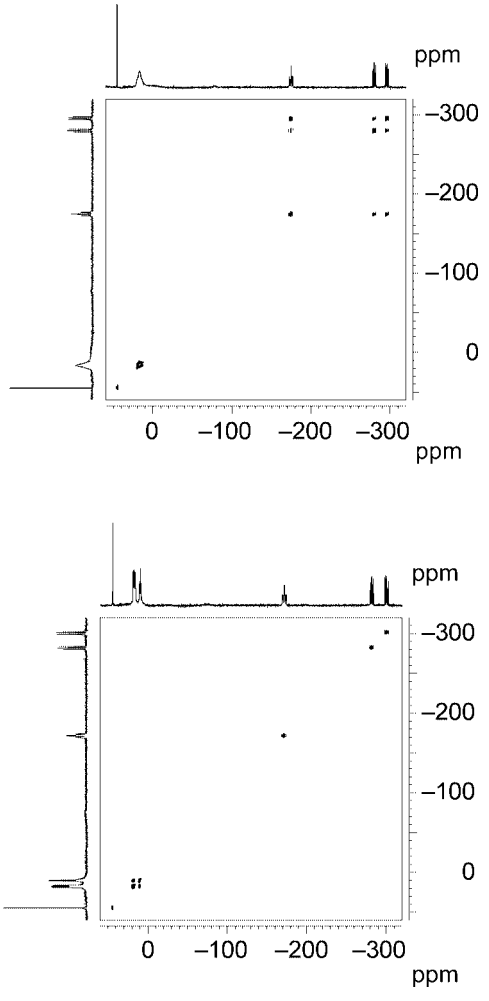

Figure 3. $^{31}P\{^{1}H\}$ EXSY spectra of **11** (CD_2Cl_2, 161.95 MHz, τ_m 0.1 s). Top, spectrum at 294 K; bottom, spectrum at 248 K.

may be accounted for by referring to two types of motion: (i) rotation of the P_3 unit with respect to the other parts of the structure (this motion, shown in Scheme 3 (*i*), involves scrambling of the Ru moiety over the cyclic system and yields the exchange peaks in the 294 K spectrum in Figure 3); and (ii) relative rotation of the {(triphos)M} moiety and the rest of the structure [Scheme 3 (*ii*)] that accounts for the exchange peaks in the EXSY spectrum at 248 K in Figure 3. The two processes are simultaneous and partly related, which makes it impossible, in view of the complex eight-nuclei spin system, to perform any reliable analysis addressing the thermodynamics of each exchange process.

The reactivity of the rhodium derivatives **9–11** has been further investigated, as the fine structure exhibited by the resonances of the "naked" atoms in the ^{31}P NMR spectra may provide more information on the solution behaviour of these dimetallic derivatives. Treatment of **9** and **11** in CH_2Cl_2 with a stoichiometric amount of PMe_3 yields the complexes $[\{(triphos)Rh\}(\mu,\eta^{3:1}\text{-}P_3)\{CpRu(PMe_3)(PR_3)\}]_6$ [R = Ph (**12**), Cy (**13**)] (Scheme 2), which form through replacement of CH_3CN by PMe_3 in the ruthenium coordination sphere. When twice as large an amount of PMe_3 is used, $[(triphos)Rh(\eta^3\text{-}P_3)]$ (**2**) and $[CpRu(PMe_3)_2(PR_3)]PF_6$ (R = Ph, Cy) are formed, which suggests an intrinsic weakness of the cyclo-P_3 coordination to the [CpRu(L)(L′)] unit. The ^{31}P NMR spectra of **12** and **13** (see the Experimental Section and Table 2) exhibit resonances for triphos, PR_3, P_F, P_M, and P_Q with similar features to those observed for **9** and **11**, besides the expected additional resonance for the PMe_3 phosphorus atom that occurs at about 2 ppm as a pseudo triplet; such multiplicity is due to fortuitous coincidence of the coupling constant to both PR_3 (R = Ph, Cy) and P_F. Interestingly, the triphos resonances, which in the parent compounds **9** and **11** appear as a broad signal, occur as a doublet of narrower multiplets, such that the

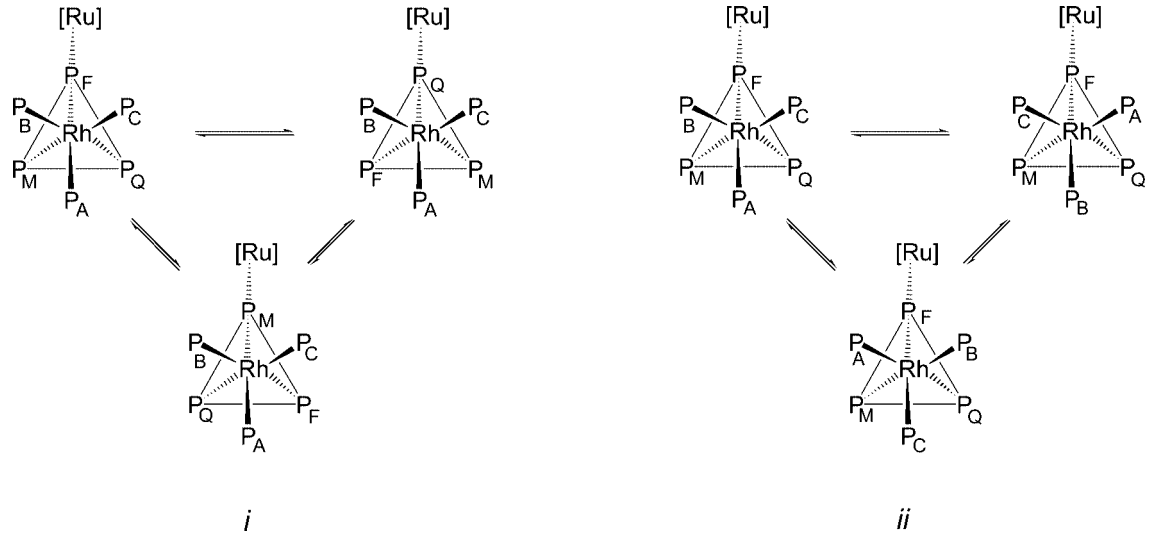

Scheme 3.

$^1J(P_{triphos}–Rh)$ is observed, see Experimental Section. Such a result points to a higher barrier for the type of motion shown in Scheme 3 (*ii*) for **12** and **13** than for **9** and **11**. This in turn may be attributed to the increased steric demand of the ruthenium fragment after replacement of the acetonitrile ligand by trimethylphosphane.

In the absence of acetonitrile, CH_2Cl_2 solutions **9** and **10** are not stable, but slowly transform to compounds with the general formula [(triphos)Rh(P_3){CpRu(PR_3)}]PF_6 [R = Ph (**14**) and Me (**15**)], by releasing the coordinated CH_3CN molecule (Scheme 2). Complexes **14** and **15** have been isolated as brown microcrystals but, in spite of repeated attempts, suitable crystals for X-ray investigations have not been obtained, so their solution structure is proposed on the basis of ^{31}P NMR spectroscopic data. The ^{31}P NMR spectra at room temperature of **14** and **15** (see Experimental Section and Table 2) exhibit resonances for triphos, PR_3, and P_F with similar shifts to those observed for **9** and **10**; the triphos and PR_3 signals are broad; those assigned to P_M and P_Q, on the other hand, appear at significantly lower field than in the parent compounds; the P_F, P_M and P_Q signals still appear as triplets and doublet of doublets, respectively, but their components are broad and only the large ^1J(P–P) coupling constants may be detected. Such data suggest that the dimetal cations in **9** and **10** have undergone minor modifications on the loss of the acetonitrile molecule to yield **14** and **15**, and that the 14e {CpRu(PR_3)} fragment interacts with the P_M and P_Q phosphorus atoms of the P_3 unit. Furthermore, the data are consistent with the rotational motion of the {(triphos)Rh} moiety and, on account of the broad resonances exhibited by the PR_3, P_F, P_M, and P_Q atoms, they point to a further process involving the CpRu(PR_3)P_3 side of the dimetal cation. A type of motion that might account for the latter aspects would be that of the ruthenium fragment, tightly bound to a P_3 phosphorus atom, that shifts between the positions of the other two, and therefore yields a dynamic $\mu,\eta^{3:1,1'}$-P_3 unit. The behaviour of **14** has been investigated at different temperatures by $^{31}P\{^1H\}$ and 2D $^{31}P\{^1H\}$ EXSY spectroscopic data. The $^{31}P\{^1H\}$ spectra show that the rates of exchange decrease on cooling, but even at the lowest reached temperature (230 K), the limiting form is not attained. The $^{31}P\{^1H\}$ EXSY spectra at 294 K and 248 K do not show cross peaks connecting either the triphos or the P_3 phosphorus atoms. These data seem to indicate that the dynamic processes occur with lower barriers than for **9** and **10**. Such a finding is consistent with the suggested geometry in solution; in fact, the ruthenium fragment, on interacting with P_M and P_Q, is expected to move slightly toward the centre of the P_3 unit, thereby releasing some steric repulsions within the cation, which are present in **9** and **10**.

Experimental Section

All reactions and manipulations were performed under dry oxygen-free argon. The solvents were purified according to standard procedures.[40] The ^1H and $^{31}P\{^1H\}$ NMR spectra at room temperature were measured on a Varian Gemini g300bb spectrometer, equipped with a variable-temperature unit, operating at 300 MHz (^1H) and 121.46 MHz (^{31}P). The variable-temperature and EXSY experiments were carried out on a Bruker Avance DRX-400 spectrometer equipped with a variable-temperature control unit accurate to ±0.1 °C and operating at 161.95 and 400.13 MHz. Chemical shifts are relative to tetramethylsilane (^1H) and to H_3PO_4 85 % (^{31}P) as external standards at δ = 0.00 ppm, with downfield values taken as positive; coupling constants are in Hertz. J(P–P) and J(P–Rh) coupling constants of **11** at low temperature were obtained by computer simulation using the gNMR program.[41] 2D NMR spectra were recorded on degassed nonspinning samples using pulse sequences suitable for phase-sensitive representations with TPPI. The 2D $^{31}P\{^1H\}$ EXSY spectra were recorded using a modified NOESY sequence with ^1H decoupling during acquisition: 400 increments of size 3 K (with 400 scans each) covering the full range in both dimensions were collected with a relaxation delay of 0.25 s and mixing times of 50, 100 and 500 ms.[42,43] Analytical data for carbon, hydrogen, nitrogen, and phosphorus were obtained from the Microanalytical Laboratory of the Department of Chemistry of the University of Firenze. The complexes [(triphos)M(η^3-P_3)] (M

= Co (**1**), Rh (**2**) and $[CpRu(CH_3CN)_2(PR_3)]PF_6$ [PR_3 = PPh_3 (**3**), PMe_3 (**4**) and PCy_3 (**5**)] were synthesized according to literature methods.[19,20,38] The ^1H NMR spectroscopic data of the dinuclear adducts **6–15** and the $^{31}P\{^1H\}$ resonances of the phosphane ligands (triphos and PR_3) are reported in this section. The uninformative ^1H signals of the aromatic protons of triphos and of the PPh_3 derivatives, occurring in the expected region (7.6–6.9 ppm), are not reported. The labelling used for the different phosphorus nuclei is defined in Scheme 2. The PF_6^- anion yields a septet centred at –143.2 [^1J(P–F) 712 Hz] in all the compounds.

Syntheses

[{(triphos)Co}(μ,η$^{3:1}$-P$_3$){CpRu(CH$_3$CN)(PPh$_3$)}]PF$_6$ (6): To a yellowish orange solution of [(triphos)Co(η^3-P$_3$)] (**1**) [132 mg, 0.17 mmol] in CH_2Cl_2 (40 mL) was added at room temperature whilst stirring one equivalent of $[CpRu(CH_3CN)_2(PPh_3)]PF_6$ (**3**) in CH_2Cl_2 (10 mL). The resulting solution was stirred for 3 h at room temperature, and during this time the colour changed to brown-red. Acetonitrile (1 mL) and toluene (10 mL) were then slowly added to yield reddish brown crystals by slowly evaporating the resulting solution at room temperature. Yield: 201 mg (85 %). $C_{66}H_{62}CoF_6NP_8Ru$ (1390.9): calcd. C 57.0, H 4.5, N 1.0 %; found C 57.1, H 4.8, N 0.9 %. ^1H NMR (CD_2Cl_2, 298 K): δ = 4.14 (s, C_5H_5, 5 H), 2.40 (br., CH_2P, 6 H), 2.20 (br. s, CH_3CN, 3 H), 1.37 (br. s, CH_3C, 3 H) ppm. $^{31}P\{^1H\}$ NMR (CD_2Cl_2, 298 K): δ = 50.2 [d, PPh_3, ^2J(PPh_3–P_F) 36.5, 1P], 34.2 (br., $P_{triphos}$, 3P) ppm.

The compounds [{(triphos)M}(μ,η$^{3:1}$-P$_3$){CpRu(CH$_3$CN)(PR$_3$)}]PF_6 [M = Co; R = Me (**7**), Cy (**8**); M = Rh; R = Ph (**9**), Me (**10**), Cy (**11**)] were prepared by the same procedure as for **6** by adding the equimolar amount of $[CpRu(CH_3CN)_2(PR_3)]PF_6$ [R = Ph (**3**), Me (**4**), Cy (**5**)] to a CH_2Cl_2 solution of [(triphos)M(η^3-P$_3$)] [M = Co (**1**), Rh(**2**)].

[{(triphos)Co}(μ,η$^{3:1}$-P$_3$){CpRu(CH$_3$CN)(PMe$_3$)}]PF$_6$ (7): Yield: 123 mg (60 %). $C_{51}H_{56}CoF_6NP_8Ru$ (1204.7): calcd. C 50.8, H 4.7, N 1.2 %; found C 50.7, H 4.8, N 1.0 %. ^1H NMR (CD_2Cl_2, 298 K): δ = 4.27 (s, C_5H_5, 5 H), 2.37 (br., CH_2P, 6 H), 2.17 (s, CH_3CN, 3 H), 1.65 (d, CH_3P, ^2J(H-P) 9.6, 9 H), 1.39 (s, CH_3C, 3 H) ppm. $^{31}P\{^1H\}$ NMR (CD_2Cl_2, 298 K): δ = 32.7 (br., $P_{triphos}$, 3P), 10.0 [d, PMe_3, ^2J(PMe_3–P_F) 46.0, 1P] ppm.

[{(triphos)Co}(μ,η$^{3:1}$-P$_3$){CpRu(CH$_3$CN)(PCy$_3$)}]PF$_6$ (8): Yield: 204 mg (85 %). $C_{66}H_{80}CoF_6NP_8Ru$ (1409.1): calcd. C 56.2, H 5.7, N 1.0 %; found C 56.1, H 5.8, N 0.8 %. ^1H NMR (CD_2Cl_2, 298 K): δ = 4.27 (s, C_5H_5, 5 H), 2.40–1.40 (br. m, C_6H_{11}, CH_2P, CH_3CN, CH_3C, 45 H) ppm. $^{31}P\{^1H\}$ NMR (CD_2Cl_2, 298 K): δ = 42.2 [d, PCy_3, ^2J(PCy_3–P_F) 39.0, 1P], 32.9 (br., $P_{triphos}$, 3P) ppm.

[{(triphos)Rh}(μ,η$^{3:1}$-P$_3$){CpRu(CH$_3$CN)(PPh$_3$)}]PF$_6$ (9): Yield: 207 mg (85 %). $C_{66}H_{62}F_6NP_8RhRu$ (1434.9): calcd. C 55.2, H 4.3, N 1.0 %; found C 55.1, H 4.5, N 0.9 %. ^1H NMR (CD_2Cl_2, 298 K): δ = 4.20 (s, C_5H_5, 5 H), 2.47 (br., CH_2P, 6 H), 2.20 (s, CH_3CN, 3 H), 1.31 (s, CH_3C, 3 H) ppm. $^{31}P\{^1H\}$ NMR (CD_2Cl_2, 298 K): δ = 51.0 [d, PPh_3, ^2J(PPh_3–P_F) 44.5, 1P], 16.9 (br., $P_{triphos}$, 3P) ppm.

[{(triphos)Rh}(μ,η$^{3:1}$-P$_3$){CpRu(CH$_3$CN)(PMe$_3$)}]PF$_6$ (10): Yield: 138 mg (65 %). $C_{51}H_{56}F_6NP_8RhRu$ (1248.7): calcd. C 49.0, H 4.5, N 1.1; found C 49.3, H 4.6, N 1.0 %. ^1H NMR (CD_2Cl_2, 298 K): δ = 4.42 (s, C_5H_5, 5 H), 2.48 (br., CH_2P, 6 H), 2.21 (s, CH_3CN, 3 H), 1.67 (d, CH_3P, ^2J(H-P) = 9.6, 9 H), 1.52 (s, CH_3C, 3 H) ppm. $^{31}P\{^1H\}$ NMR (CD_2Cl_2, 298 K): δ = 16.8 (br., $P_{triphos}$, 3P), 9.8 [d, PMe_3, ^2J(PMe_3–P_F) 49.5, 1P] ppm.

[{(triphos)Rh}(μ,η$^{3:1}$-P$_3$){CpRu(CH$_3$CN)(PCy$_3$)}]PF$_6$ (11): Yield: 210 mg (85 %). $C_{66}H_{80}F_6NP_8RhRu$ (1453.0): calcd. C 54.5, H 5.5, N 1.0, P 17.0 %; found C 54.3, H 5.7, N 0.8, P 16.8 %. ^1H NMR (CD_2Cl_2, 298 K): δ = 4.23 (s, C_5H_5, 5 H), 2.40–1.4 (br. m, C_6H_{11}, CH_2P, CH_3CN, CH_3C) ppm. $^{31}P\{^1H\}$ NMR (CD_2Cl_2, 298 K): δ = 44.4 [d, PCy_3, ^2J(PCy_3–P_F) 44.5, 1P], 16.0 (br., $P_{triphos}$, 3P) ppm.

[{(triphos)Rh}(μ,η$^{3:1}$-P$_3$){CpRu(PMe$_3$)(PPh$_3$)}]PF$_6$ (12): To an orange solution of [{(triphos)Rh}(μ,η$^{3:1}$-P$_3$){CpRu(CH$_3$CN)-(PPh$_3$)}]PF_6 (**9**) [143 mg, 0.10 mmol] in CH_2Cl_2 (20 mL) was added at room temperature whilst stirring an equimolar amount of neat PMe_3. The resulting solution was stirred for 2 h; toluene (15 mL) was then slowly added; reddish-orange crystals were obtained by slowly evaporating the resulting solution at room temperature. Yield: 200 mg (80 %). $C_{67}H_{68}F_6P_9RhRu$ (1469.9): calcd. C 54.7, H 4.7 %; found C 54.5, H 4.6 %. ^1H NMR (CD_2Cl_2, 298 K): δ = 4.34 (s, C_5H_5, 5 H), 2.41 (br., CH_2P, 6 H), 1.52 (s, CH_3C, 3 H), 1.31 [d, CH_3P, ^2J(H–P) = 9.3, 9 H] ppm. $^{31}P\{^1H\}$ NMR (CD_2Cl_2, 298 K): δ = 50.2 [dd, PPh_3, ^2J(PPh_3–PMe_3) 41.5, ^2J(PPh_3–P_F) 36.5, 1P], 16.5 [br. d, $P_{triphos}$, ^1J($P_{triphos}$–Rh) 130.5, 3P], 2.2 [t, PMe_3, ^2J(PMe_3–P_F) 42.0, 1P] ppm.

[{(triphos)Rh}(μ,η$^{3:1}$-P$_3$){CpRu(PMe$_3$)(PCy$_3$)}]PF$_6$ (13): Complex **13** was prepared as described above for **12** by using **11** instead of **9**. Yield: 202 mg (80 %). $C_{67}H_{86}F_6P_9RhRu$ (1488.1): calcd. C 54.1, H 5.8 %; found C 54.2, H 5.9 %. ^1H NMR (CD_2Cl_2, 298 K): δ = 4.32 (s, C_5H_5, 5 H), 2.40–1.30 (br. m, C_6H_{11}, CH_2P, CH_3C, 42 H), 1.25 [d, CH_3P, ^2J(H–P) 8.7, 9 H] ppm. $^{31}P\{^1H\}$ NMR (CD_2Cl_2, 298 K): δ = 46.0 [t, PCy_3, ^2J(PCy_3–PMe_3) = ^2J(PCy_3–P_F) 39.0, 1P], 15.0 [br. d, $P_{triphos}$, ^1J($P_{triphos}$–Rh) 120.0, 3P], 2.1 [t, PMe_3, ^2J(PMe_3–P_F) 40.0, 1P] ppm.

[{(triphos)Rh}(μ,η$^{3:1,1'}$-P$_3$){CpRu(PPh$_3$)}]PF$_6$ (14): [(triphos)Rh(η^3-P$_3$)] (**2**) and $[CpRu(CH_3CN)_2(PPh_3)]PF_6$ (**3**) were reacted as described for **9** avoiding the subsequent addition of acetonitrile. Brown microcrystals were obtained by adding only toluene, and slowly concentrating the resulting solution. Yield: 154 mg (65 %). $C_{64}H_{59}F_6P_8RhRu$ (1393.8): calcd. C 55.1, H 4.3, P 17.8 %; found C 55.2, H 4.4, P 17.6 %. ^1H NMR (CD_2Cl_2, 298 K): δ = 4.02 (s, C_5H_5, 5 H), 2.37 (br., CH_2P, 6 H), 1.53 (s, CH_3C, 3 H) ppm. $^{31}P\{^1H\}$ NMR (CD_2Cl_2, 298 K): δ = 48.4 (br. s, PPh_3, 1P), 15.5 [dq, $P_{triphos}$, ^1J($P_{triphos}$–Rh) 132.0, ^2J($P_{triphos}$–$P_{cyclo\text{-}P3}$) 21.0, 3P] ppm.

[{(triphos)Rh}(μ,η$^{3:1,1'}$-P$_3$){CpRu(PMe$_3$)}]PF$_6$ (15): Brown microcrystals of **15** were obtained as described above for **14** by reacting [(triphos)Rh(η^3-P$_3$)] (**2**) and $[CpRu(CH_3CN)_2(PMe_3)]PF_6$ (**4**) in a 1:1 ratio in CH_2Cl_2. Yield: 123 mg (60 %). $C_{49}H_{53}F_6P_8RhRu$ (1207.6): calcd. C 48.7, H 4.4, P 20.5 %; found C 48.9, H 4.4, P 20.2 %. ^1H NMR (CD_2Cl_2, 298 K): δ = 4.15 (s, C_5H_5, 5 H), 2.37 (br., CH_2P, 6 H), 1.53 (s, CH_3C, 3 H), 1.50 [d, CH_3P, ^2J(H–P) 9.3] ppm. $^{31}P\{^1H\}$ NMR (CD_2Cl_2, 298 K): δ = 16.2 [dm, $P_{triphos}$, ^1J($P_{triphos}$–Rh) 127.0, 3P], 8.0 (m, PMe_3, 1P) ppm.

Crystal Structure Determination

Obtaining crystals suitable for X-ray analyses on these compounds proved to be difficult; a data set could only be collected with a very small crystal of **6**, grown from a diluted CH_2Cl_2/CH_3CN/C_7H_8 solution, which gave relatively low-angle reflections. Data were collected at room temperature with a Bruker CCD diffractometer, equipped with Göbel mirrors and mounted on a rotating-anode generator, using Cu-K_α radiation (λ = 1.5418 Å). Cell constants were obtained by least-squares refinement of the setting angles of 791 reflections in the range $7° < 2\theta < 55°$. Crystallographic data and details on the structure determination and refinement procedure are summarised in Table 4. Although limited absorption effects were expected, in view of the small size of the crystal, a correction for absorption was applied with SADABS,[44] in an attempt to reduce the effects of absorption by the glass fibre, which caused

high R_{int} values. The structure was solved by direct methods with SIR-97[45] and was extended and refined on F^2 with SHELXL-97.[46] In addition to the ions forming the unit formula of **6**, two solvate toluene molecules were located in the asymmetric unit. In the final sets of the refinement cycles, the metal, P and F atoms, as well as the three outermost C atoms of each phenyl ring − those of the cyclopentadiene ligand and of the two solvent molecules − were refined anisotropically, with soft isotropic restraints on temperature factors of the C atom. The phenyl, cyclopentadiene, and toluene rings were refined as rigid groups, and a constraint was also applied on the C–CH_3 distance of one toluene molecule. Hydrogen atoms were in calculated positions, riding on the respective carrier atom, with $U_H = 1.2U_C^{eq}$ ($U_H = 1.5U_C^{eq}$ for methyl hydrogens). A small damping factor was applied. Features in the final difference synthesis were low and devoid of chemical meaning. Computer programs used included PARST[47] for geometry calculations, and ORTEP[48,49] for graphics.

Table 4. Crystal data and structure refinement parameters for **6**.

Empirical formula	$C_{80}H_{78}CoF_6NP_8Ru$
Formula weight	1575.19
Crystal system	orthorhombic
Space group	*Pcab* (no. 61)
a [Å]	22.138(4)
b [Å]	22.955(5)
c [Å]	30.038(7)
V [Å^3]	15265(6)
Z	8
$D_{calcd.}$ [g cm^{-3}]	1.371
μ [mm^{-1}]	5.364
Transmission factors range	0.549–1.000
Crystal size [mm]	0.05 × 0.08 × 0.40
F(000)	6480
θ range [°]	2.94–37.56
Index ranges	$-17 \le h \le 17$, $-18 \le k \le 17$, $-23 \le l \le 23$
Reflections collected	33678
Independent reflections	3873 [$R_{int} = 0.322$]
Independent observed reflections	1507 [$I > 2\sigma(I)$]
Restraints/Parameters	313/572
Final *R* indices [$I > 2\sigma(I)$]	$R_1 = 0.056$, $wR_2 = 0.071$
R indices (all data)	$R_1 = 0.199$, $wR_2 = 0.093$
Goodness of fit on F^2 (all data)	0.806
Largest diff. peak and hole [e·Å^{-3}]	0.316 to –0.250

CCDC-244899 contains the supplementary crystallographic data for this paper. These data can be obtained free of charge from The Cambridge Crystallographic Data Centre via www.ccdc.cam.ac.uk/data_request/cif.

Acknowledgments

We acknowledge financial support by the Ministero dell'Università e della Ricerca Scientifica e Tecnologica (Rome) and by the European Commission through the program INTAS (00–00018). Thanks are also expressed to THERMPHOS International, Vlissingen, NL for supporting this research.

[1] M. Di Vaira, P. Stoppioni, *Coord. Chem. Rev.* **1992**, *120*, 259–279.
[2] J. Wachter, *Angew. Chem. Int. Ed. Engl.* **1998**, *37*, 751–768.
[3] O. J. Scherer, *Acc. Chem. Res.* **1999**, *32*, 751–762.
[4] M. P. Ehses, A. Romerosa, M. Peruzzini, *Top. Curr. Chem.* **2002**, *220*, 107–140.
[5] B. P. Johnson, G. Balazs, M. Scheer, *Top. Curr. Chem.* **2004**, *232*, 1–23.
[6] O. J. Scherer, G. Berg, G. Wolmershäuser, *Chem. Ber.* **1995**, *128*, 635–639.
[7] A. Barth, G. Huttner, M. Fritz, L. Zsolnai, *Angew. Chem. Int. Ed. Engl.* **1990**, *29*, 929–931.
[8] O. J. Scherer, J. Braun, P. Walther, G. Wolmershäuser, *Chem. Ber.* **1992**, *125*, 2661–2665.
[9] O. J. Scherer, T. Mohr, G. Wolmershäuser, *J. Organomet. Chem.* **1997**, *529*, 379–385.
[10] O. J. Scherer, G. Schwarz, G. Wolmershäuser, *Z. Anorg. Allg. Chem.* **1996**, *622*, 951–957.
[11] G. Friedrich, O. J. Scherer, G. Wolmershäuser, *Z. Anorg. Allg. Chem.* **1996**, *622*, 1478–1486.
[12] O. J. Scherer, G. Berg, G. Wolmershäuser, *Chem. Ber.* **1996**, *129*, 53–58.
[13] M. Di Vaira, M. P. Ehses, M. Peruzzini, P. Stoppioni, *J. Organomet. Chem.* **2000**, *593–594*, 127–134.
[14] O. J. Scherer, B. Werner, G. Heckmann, G. Wolmershäuser, *Angew. Chem. Int. Ed. Engl.* **1991**, *30*, 553–555.
[15] O. J. Scherer, J. Schwalb, G. Wolmershäuser, *New J. Chem.* **1989**, *13*, 399–402.
[16] O. J. Scherer, R. Winter, G. Wolmershäuser, *Z. Anorg. Allg. Chem.* **1993**, *619*, 827–835.
[17] M. Scheer, E. Leiner, P. Kramkowski, M. Schiffer, G. Baum, *Chem. Eur. J.* **1998**, *4*, 1917–1923.
[18] J. E. Davies, M. J. Mays, P. R. Raithby, G. P. Shields, P. K. Tompkin, A. D. Woods, *J. Chem. Soc. Dalton Trans.* **2000**, 1925–1930.
[19] C. A. Ghilardi, S. Midollini, A. Orlandini, L. Sacconi, *Inorg. Chem.* **1980**, *19*, 301–306.
[20] C. Bianchini, C. Mealli, A. Meli, L. Sacconi, *Inorg. Chim. Acta* **1979**, *37*, L543–L544.
[21] C. Mealli, S. Midollini, S. Moneti, L. Sacconi, *Cryst. Struct. Commun.* **1980**, *9*, 1017–1022.
[22] M. Di Vaira, L. Sacconi, P. Stoppioni, *J. Organomet. Chem.* **1983**, *250*, 183–195.
[23] M. Di Vaira, M. Peruzzini, P. Stoppioni, *J. Chem. Soc. Dalton Trans.* **1984**, 359–364.
[24] M. Di Vaira, P. Innocenti, S. Moneti, M. Peruzzini, P. Stoppioni, *Inorg. Chim. Acta* **1984**, *83*, 161–165.
[25] M. Di Vaira, M. Peruzzini, P. Stoppioni, *Polyhedron* **1986**, *5*, 945–950.
[26] M. Di Vaira, L. Sacconi, *Angew. Chem. Int. Ed. Engl.* **1982**, *21*, 330–342.
[27] M. Di Vaira, P. Stoppioni, M. Peruzzini, *Polyhedron* **1987**, *6*, 351–382.
[28] S. Midollini, A. Orlandini, L. Sacconi, *Angew. Chem. Int. Ed. Engl.* **1979**, *18*, 81–82.
[29] M. Di Vaira, D. Rovai, P. Stoppioni, *Polyhedron* **1990**, *9*, 2477–2481.
[30] M. Di Vaira, M. Peruzzini, P. Stoppioni, *J. Chem. Soc. Dalton Trans.* **1990**, 109–113.
[31] M. Di Vaira, P. Stoppioni, *Polyhedron* **1994**, *13*, 3045–3051.
[32] M. Di Vaira, S. Moneti, M. Peruzzini, P. Stoppioni, *J. Organomet. Chem.* **1984**, *266*, C8–C10.
[33] M. Di Vaira, P. Stoppioni, M. Peruzzini, *Acta Crystallogr. Sect. C* **1987**, *43*, 1284–1287.
[34] M. Di Vaira, M. P. Ehses, P. Stoppioni, M. Peruzzini, *Inorg. Chem.* **2000**, *39*, 2199–2205.
[35] W. Luginbühl, P. Zbinden, P. A. Pittet, T. Armbruster, H. B. Bürgi, A. E. Merbach, A. Ludi, *Inorg. Chem.* **1991**, *30*, 2350–2355.
[36] G. Capozzi, L. Chiti, M. Di Vaira, M. Peruzzini, P. Stoppioni, *J. Chem. Soc. Chem. Commun.* **1986**, 1799–1800.
[37] M. Di Vaira, S. Seniori Costantini, F. Mani, M. Peruzzini, P. Stoppioni, *J. Organomet. Chem.* **2004**, *689*, 1757–1762.

[38] E. Rüba, W. Simanko, K. Mauthner, K. M. Soldouzi, C. Slugovc, K. Mereiter, R. Schmid, K. Kirchner, *Organometallics* **1999**, *18*, 3843–3850.
[39] A. Bax, *Two-dimensional Nuclear Magnetic Resonances in Liquids*, Delft University Press, Dordrecht, The Netherlands, **1982**.
[40] D. D. Perrin, W. L. F. Armarego, *Purification of Laboratory Chemicals*, 3rd ed., Pergamon, New York, **1988**.
[41] P. H. M. Budzelaar, *gNMR V4.0*, Cherwell Scientific Publishing, Copyright **1995**–**1997** Ivory soft.
[42] V. Sklenar, H. Miyashiro, G. Zon, H. T. Miles, A. Bax, *FEBS Lett.* **1986**, *208*, 94–98.
[43] J. Jeener, B. H. Meier, P. Bachmann, R. R. Ernst, *J. Chem. Phys.* **1979**, *71*, 4546–4553.
[44] G. M. Sheldrick, *SADABS, Program for Empirical Absorption Corrections*, University of Göttingen, Göttingen, Germany, **1986**.
[45] A. Altomare, M. C. Burla, M. Camalli, G. L. Cascarano, C. Giacovazzo, A. Guagliardi, A. G. Moliterni, G. Polidori, R. Spagna, *J. Appl. Crystallogr.* **1999**, *32*, 115–119.
[46] G. M. Sheldrick, *Shelxl 97, Program for Crystal Structure Refinement*, University of Göttingen, Göttingen, Germany, **1997**.
[47] PARST : M. Nardelli, *J. Appl. Crystallogr.* **1995**, *28*, 659.
[48] C. K. Johnson, ORTEP, Report ORNL–5138, Oak Ridge National Laboratory, Oak Ridge, TN.
[49] L. J. Farrugia, *J. Appl. Crystallogr.* **1999**, *32*, 837–838.
Received: October 8, 2004

